# MASW to Map Shear-Wave Velocity of Soil

Choon B. Park and Richard D. Miller

Kansas Geological Survey
University of Kansas
1930 Constant Avenue, Campus West
Lawrence, Kansas 66047-3726

Final Report to

Richard W. Smith, P.E.
Camp Dresser and McKee, Inc.
11811 NE 1st Street, Suite 201
Bellevue, WA 98005

Open-file Report 2004-30 May 17, 2004

# MASW to Map Shear-Wave Velocity of Soil

by

Choon B. Park and Richard D. Miller
Kansas Geological Survey
University of Kansas
1930 Constant Avenue, Campus West
Lawrence, Kansas 66047-3726
Tel: 785-864-2162  Fax: 785-864-5317
Emails: park@kgs.ku.edu, rmiller@kgs.ku.edu

KGS Project Number: IN34290

Final Report to

Richard W. Smith, P.E.
Senior Geotechnical Engineer
Camp Dresser and McKee, Inc.
11811 NE 1st Street, Suite 201
Bellevue, Washington 98005
Tel: 425-453-8383 / Fax: 425-646-9523
Email: smithrw@cdm.com

KGS Open-file Report 2004-30

May 17, 2004

## ABSTRACT

Two surveys using the multichannel analysis of surface waves method were conducted over a soil site in Tacoma Water's Green River Facility, Washington, at the proposed future site of a chemical treatment facility. The purpose of these surveys was to map shear-velocity (Vs) distribution before and after Deep Dynamic Compaction operations. It is generally accepted that soil stiffness is proportional to shear velocity. Soil at this site consisted of a very heterogeneous mixture of gravel and cobbles in a sand-and-silt matrix. Results from each survey are represented by 2-D Vs maps representative of soil characteristics below the surveyed lines. From each survey two Vs maps were produced: one map was constructed from dispersion curves analyzed subjectively, whereas a second map was constructed from the same dispersion curves analyzed objectively. The major difference was the use of automatic, computer-aided analysis for the objective analysis.

## INTRODUCTION

Soil stiffness is one of the critical material parameters considered during an early stage of most geotechnical construction. It is related directly to the stability of structural load, especially as it relates to possible earthquake hazard. Soil lacking sufficient stiffness for a given load can experience a significant reduction in strength under earthquake shaking resulting in liquefaction, a condition responsible for tremendous amounts of damage from earthquakes around the world (Richart et al., 1970). Minimal soil stiffness criteria are, therefore, strictly enforced for construction of buildings in earthquake-prone areas. This is especially the case if building damage may result in a significant threat to public safety.

Traditionally, several geotechnical or geophysical methods have been used to quantify soil stiffness. These include the cone penetration test (CPT) (Lunne, 1997) and down-hole seismic (Dobrin and Savit, 1988) methods. CPT is an in-situ method that evaluates stiffness by measureing resistance to the penetration of a probe. Down-hole seismic methods measure travel times to establish seismic velocities that are linked to the stiffness. Among all other elastic parameters of materials, shear-wave velocity (Vs) is the best indicator of stiffness (Bullen, 1963). CPT and down-hole methods require drilling holes for insertion of probes and give stiffness information only representative of a localized volume very near the hole. Shear-wave down-hole methods are generally considered less reliable because of difficulties in generating pure shear waves and processing acquired data.

Recently, surface wave methods have become the seismic techniques most often used to estimate the Vs structure of soil because of their non-invasive nature and greater efficiency in data acquisition and processing (Miller et al., 1999; Stokoe et al., 1994). Propagation velocity (called phase velocity) of surface waves is frequency (or wavelength) dependent (this property is called dispersion). The dispersiveness of soils is determined mainly by the vertical variation in Vs. By recording fundamental-mode Rayleigh waves propagating horizontally and directly from the seismic source to receiver, the dispersive properties directly beneath the source and receiver spread can be measured and usually represented by a curve (called dispersion curve) depicting variation of phase velocities with frequency. This curve is then used to estimate the vertical variation of Vs (called 1-D Vs profile) through a process called inversion.

Although generally thought to be a relatively easy seismic method to use, several complications may interfere with the effectiveness of the surface-wave method, especially if improper acquisition or processing (or both) techniques are used. Higher-mode surface wave energy and body wave direct arrivals can often interfere with the generation of the fundamental-mode dispersion curve. In some cases where Vs changes rapidly with depth, recorded surface waves can contain significant amounts of leaky modes whose energy dissipates rapidly into the medium, leaving no fundamental mode energy. If not properly identified, leaky modes can be misinterpreted as normal modes of surface waves.

The multichannel analysis of surface waves (MASW) method (Park et al., 1999a; Xia et al., 1999; Miller et al., 1999) utilizes pattern-recognition techniques made possible by the multichannel recording and processing approaches. MASW employs multiple receivers (geophones) equally spaced along a linear survey line with seismic waves generated by an impulsive source (like a sledgehammer) and propagated along the receiver line where they are recorded synchronously. This approach allows recognition of the various propagation characteristics of the seismic wavefield (Figure 1). Pattern recognition possible with multichannel recording has long been utilized in seismic exploration for natural resources (Telford et al., 1976).

The main aspect of the seismic wavefield capitalized on by MASW is the frequency dependency of phase velocities (dispersion property) for all horizontally propagating seismic waves. In fact, the dispersive properties are first imaged (rather than calculated) using an objecttive wavefield transformation method that delineates the property using a proper pattern-recognition technique (Park et al., 1998) (Figure 2). The dispersion characteristics of the fundamental mode Rayleigh waves are then identified in the image and a corresponding signal curve is extracted and used in the inversion step. A 1-D Vs profile is obtained from the inversion and this profile best represents the vertical Vs structure at the middle of the receiver spread used for the analysis. Because of this enhanced effectiveness in data processing provided by multiple-receiver recording, one measurement from one impact and one source-receiver (SR) configuration is usually sufficient to produce a 1-D Vs profile. By subsequently moving the same SR configuration along a preset survey line, multiple measurements can be made, each producing a 1-D Vs profile that, when all gathered together, can be used to construct a 2-D Vs map (Figure 3). This 2-D Vs map represents a cross-sectional view of Vs distribution below the survey line.

Construction at Tacoma Water's Green River facility required knowledge of soil stiffness both before and after mechanical compaction (Figure 4). With a very heterogeneous soil consisting of a mix of gravel and cobbles in a sand-and-silt matrix, Deep Dynamic Compaction (DDC) was planned to prepare the site for construction. DDC operations involve the dropping of a 5 to 30 ton weight from heights of 30 to 120 ft with the hope of significantly increasing the stiffness property of soil at the site. Two MASW surveys were performed before and after the DDC operations. The pre-compaction survey was performed on September 10 and the post-compaction survey on November 5, 2003. Maximum depth of investigation was chosen to be around 25 ft.

## GENERAL PROCEDURE WITH THE MASW METHOD

MASW is a comparatively simple seismic method. Multiple receivers are equally spaced along a linear survey line (Figure 1). Considering the frequency-with-depth dependency of surface waves and the response characteristics of geophones, low-frequency (4.5 Hz) geophones are normally used as receivers and a heavy impact seismic source like a 16-lb sledgehammer can produce a broadband, relatively low-frequency signal. Distance ($x_1$) between source and nearest-receiver-station (called source offset) is chosen to minimize near-field effects caused by excessive stress-strain relationship from the impact source (Park et al., 2002; 2001). This source offset is usually chosen to be about the same as the maximum depth of investigation. However, situations do exist where source-to-receiver offsets less than the depth of interest are appropriate (Park et al., 1999a). Receiver spacing ($dx$) is chosen to avoid any possible spatial aliasing of the shortest wavelength recorded and to maximize the effectiveness of dispersion analysis (Park et al., 2001). Total length of receiver spread ($x_T$) determines the farthest offset and receiver spacing and needs to be short enough that strong body and higher-mode surface waves, usually dominant at far offsets, do not interfere with fundamental-mode dispersion curve analysis. Specific source-receiver (SR) configurations are defined by source offset, receiver spacing, and receiver spread. A measurement is a multichannel record (called a shot gather) resulting from one or more seismic impact(s) recorded at a single point by a fixed receiver spread. The vibration history related to the source-generated seismic wavefield is measured by each geophone within the spread and is represented by a time series referred to as a trace (Figure 1). From each measurement comes a single 1-D Vs profile of the earth materials directly beneath the spread. In a survey designed to generate a 2-D Vs map, a chosen SR configuration is uniformly and consistently moved by a given distance (called source interval, which is usually a multiple of the individual receiver spacing) along the survey line, making measurements at each shot station until the target area has been surveyed. This moving-spread style of data acquisition is called a roll-along mode (Sheriff and Geldart, 1982).

The general scheme of data processing consists of following steps:

1. discard (edit) noisy shot gathers;
2. convert raw seismic data (SEG-2) into processing format (KGS), combining all shot gathers to be processed into a single file;
3. assign field geometry and recompile into the roll-along mode data set;
4. view all shot gathers to assess general signal-to-noise (S/N) ratio;
5. select representative shot gathers from the beginning, middle, and end of survey line and process them for dispersion images to determine optimum ranges for frequency and phase velocity;
6. dispersion-curve analysis for all the shot gathers;
7. inversion analysis for all the dispersion curves analyzed; and
8. construct 2-D Vs map from the inversion results by using an appropriate 2-D interpolation scheme.

Shot gathers with triggering errors or with S/N below acceptable thresholds are discarded. All remaining gathers are then converted and combined into a single file with sequentially increasing field file numbers (record number). Station numbers for source and receivers

and the receiver spacing are assigned to each record in the combined file. Then, all the geometry-encoded records are recompiled into the equivalent roll-along mode data set by discarding certain portions of traces in each record. All the records are then viewed to generally assess data quality (S/N). Next, several records are selected from several different locations along the survey line and their dispersion characteristics examined using the imaging method (Park et al., 1998). During this step, an optimum range of frequencies and phase velocities is chosen which is used to guide the processing of all the records in the data set. Each record is analyzed to generate a dispersion image (called overtone image) with the fundamental-mode dispersion trend identified and a signal dispersion curve extracted based on the image identified. Once all the necessary dispersion curves have been extracted, they are inverted to generate one 1-D Vs profile from each dispersion curve. The resulting Vs profile is assigned the station location in the middle of the receiver spread. When all 1-D Vs profiles are generated for all dispersion curves, a 2-D interpolation scheme (for example, bilinear or Kriging scheme) is used to construct the final 2-D Vs map.

## DATA ACQUISITION

The pre-compaction seismic survey was performed on September 10 and the post-compaction survey on November 5, 2003 (Figure 4). The post-compaction profile was moved slightly relative to the pre-compaction line after reassessing all available information.

### Pre-Compaction Survey (Line 2000)

A receiver spacing (*dx*) (therefore station spacing) of 2 ft was chosen to insure any extremely low (usually lower than 200 ft/sec) Vs in the soil was properly measured. A 12 ft (6 *dx*) source offset ($x_1$) was chosen to account for the near-field effects. A source interval of 4 ft (2 *dx*) was selected after considering possible degree of horizontal heterogeneity of Vs in the area. One complete receiver spread consisted of 72 (4.5 Hz) geophones connected by three 24-takeout cables. Three 24-channel seismographs (Geometrics Geodes) were connected individually to each cable and all three were configured to become one 72-channel acquisition system by connecting them through Ethernet connections to a notebook computer. A 16-lb sledgehammer was used as the energy source and one shot gather was recorded for each vertical impact of the hammer. A small rectangular (6 inch by 6 inch) aluminum plate was used as a strike plate to maximize energy transfer between the hammer and ground. By using a 72-channel recording system it was possible to simulate a conventional roll-along mode acquisition system without a roll-along switch and with the additional advantage of diversity in data manipulation possibilities post-acquisition.

The first shot location was at station 1999 and first geophone planted at station 2005, resulting in a source offset (6 *dx*) of 12 ft. Then, the source location moved by two stations (2 *dx*) to 2001, leaving the entire 72-receiver spread stationary until the source had been moved 48 times. This incremental source movement with the given SR configuration allows simulation of a 24-channel roll-along acquisition mode by simply selecting the correct 24 channels from each 72-channel record during the early stage of data processing (step 3). After 48 shots were acquired, the first 48 receivers were moved to the end of the receiver spread, redeployed, and seismographs reconfigured to define this new 72-channel spread. Shot points started at station

1999 and continued to station 2289, moving in two-station increments. A sampling interval of 0.5 ms was used over a total recording time of 1000 ms. Each shot (single impact) was recorded individually without vertical stacking. No acquisition filters were used.

The ground condition was extremely soft and rough for approximately the first half of the survey line. A single impact would drive the striker plate as much as one foot into the soil. This part of the survey line resulted in shot gathers with complicated dispersion characteristics, usually lacking coherency. The ground firmed a bit and the surface smoothed some for the second half of the survey line.

All pre-compaction shot gathers collected are displayed in Appendix I. The first 500 ms of each shot gather is displayed and the relative location of the receiver spread within the survey area is indicated in a rectangular inset.

**Post-Compaction Survey (Line 4000)**

The placement of the survey line was slightly different from the pre-compaction line, a decision made after reassessing the relative significance of Vs evaluation within the site. For the most part, the same source-receiver configuration and recording parameters were used as in the pre-compaction survey. However, the source increment was chosen to be a 4-station interval (8 ft) rather than the 2-station interval (4 ft) used during the pre-compaction survey. This decision was made based on the horizontal heterogeneity of soil evaluated from the pre-compaction data. Source stations ranged from 3996 to 4239 (Figure 4).

The ground condition was extremely soft and rough for most of the survey line. Although it gradually became firmer and smoother toward the second half of the line, conditions in general were softer and rougher than in the pre-compaction survey, possibly due to the disturbance caused by compaction operations. Although the top portion of the ground was slightly frozen during the early stage of the survey, it melted and became very muddy in the middle of the day as the acquisition got closer to the second half of the line.

All post-compaction shot gathers collected are displayed in Appendix II. The first 500 ms of each shot gather is displayed and the relative location of the receiver spread within the survey area is indicated on a rectangular inset.

## DATA PROCESSING — DISPERSION ANALYSIS

Several shot gathers were chosen from the front, middle, and end portions of the survey line and were used for preliminary processing to assess the optimum ranges of frequency and phase velocity used during the overtone analysis. Using the defined ranges, each shot gather was transformed into the overtone image using the 2-D wavefield transformation method. Then the fundamental-mode dispersion trend was identified and the signal dispersion-curve was extracted. This entire procedure, including dispersion analysis, was accomplished using surface-wave processing software (*SurfSeis* v. 1.5, 2003) developed at the Kansas Geological Survey.

## Pre-Compaction Analysis

Overtone images of all pre-compaction shot gathers collected are displayed in Appendix III. Images obtained from shot gathers (approximately records 2001 to 2030) collected across the first one-third of the line contain energy trends that are so complicated any coherent signal that could be identified as fundamental-mode surface waves is terribly obscured by noise. This is likely due to the extremely soft soil condition at the ground surface either preventing the generation of stabilized surface waves or imparting most of the seismic energy in the form of leaky mode surface waves and normal compressional body waves. Coherent energy trends are identified on subsequent records from approximately 2034 to 2045. This coherent energy trend occurs in the frequency range of 20-50 Hz with a phase-velocity range of 250-1250 ft/sec. This coherent energy wavetrain starts breaking up on the subsequent records (2046 to 2061, approximately). Another coherent trend starts to appear around 2063 possessing a significantly different phase velocity range (200-500 ft/sec). This changing energy arrival pattern from coherent to broken and then back to coherent indicates that there is a significant horizontal seismic velocity (Vs) change with the more chaotic zones. In general, low-velocity dispersion curves are maintained throughout the high station number end of the profile (records from 2062 to 2155).

After examination of the corresponding overtone image, attempts were made using *SurfSeis* (2003) to extract one fundamental-mode dispersion curve from each shot gather. First, a reference point was assigned on the dispersion trend where the high confidence peak appears in the energy accumulation. Next, starting and ending frequencies were selected to define the frequency range of the extracted dispersion curve. A frequency interval of 1 Hz was selected for each dispersion curve extraction. Dispersion curves extracted automatically by the program usually followed the identified trend. However, it sometimes contained erroneous portions caused by broken coherency, adjacent higher mode trends (Park et al., 1999b), or both. In this case, those portions were manually edited, replacing them with the subjectively determined values (Figure 5). This manual editing often involved enlarging the analyzed frequency range. Those shot gathers (for example, record 2001) whose overtone images showed no discernible trend in the fundamental-mode Rayleigh waves were not included in the analysis.

Two dispersion-curve extraction passes were made. One extraction (to be called "Subjective" analysis) involved as much subjective judgment as possible (Figure 6a). This was aimed at maximizing the total number of curves extracted in the defined frequency range. This type of extraction involved examination of overtone images several times with different processing parameters and display. Another pass of extraction (to be called "Objective" analysis) involved only those shot gathers whose overtone images show a trend that could be clearly and obviously identified as the fundamental-mode curve (for example, record 2133) (Figure 6b). Dispersion curves extracted from each pass of analysis demonstrate this procedure (Figure 7).

## Post-Compaction Analysis

Overtone images of all post-compaction shot gathers collected are displayed in Appendix IV. The general procedure used to extract dispersion curves was the same as that described in the pre-compaction case previously outlined. Two passes of Subjective and Objective analyses were made for the entire data set (Figure 8).

## DATA PROCESSING — INVERSION FOR Vs PROFILES

Each dispersion curve was inverted using an iterative inversion algorithm (incorporated into *SurfSeis*) (Xia et al., 1999) to produce a one-dimensional (1-D) Vs profile in which vertical variation of Vs at a certain location in the survey line is represented by a layer model (Figure 9). The surface location of a 1-D Vs profile is defined as the middle point of the receiver spread used during the dispersion-curve extraction. A 10-layer model with a varying thickness (increasing thickness with depth) was used at this site. This layer model was selected by the *SurfSeis* program based on the relationship between phase velocities and wavelengths calculated from dispersion curves. Iterative inversion processes stopped when one of three criteria was met: 1) when overall root-mean-square error (RMS-E) dropped below ten, or 2) when total iteration reached thirty, or 3) when changes of RMS-E remained less than five percent for successive five iterations (*SurfSeis* Users' Manual, 2003).

### Pre-Compaction 2-D Vs Map

Two 2-D Vs maps were constructed: one (the Subjective Vs map) (Figure 10a) using all the Subjective dispersion curves and their calculated 1-D Vs profiles and another (the Objective Vs map) (Figure 11a) obtained by using 1-D Vs profiles from all the Objective curves. Location of each 1-D Vs profile used for the construction of the map is indicated by a triangular mark at the bottom of map. Corresponding RMS-E maps of Figures 10b and 11b, respectively, indicate relative level of confidence (the smaller RMS-E, the higher confidence) in the 2-D Vs maps. Since this confidence was calculated purely from the numerical perspectives, they should be used with a care.

### Post-Compaction 2-D Vs Map

The same procedure was used during post-compaction processing as described for pre-compaction processing to produce two 2-D Vs maps: the Subjective (Figure 12a) and the Objective (Figure 13a). Corresponding RMS-E maps are also displayed in Figures 12b and 13b, respectively.

## DISCUSSION

Comparing Vs maps from Subjective and Objective analyses, Objective Vs maps are slightly smoothed versions of the Subjective ones. This is because fewer data points were used during the inversion process. Therefore, the Objective maps have a lesser degree of resolution in both horizontal and vertical directions. For example, the abrupt and unrealistic horizontal step-like change observed near station 2120 in the pre-compaction Objective Vs map (Figure 11a) is due to the spatial gap between adjacent dispersion curves used for the inversion process. However, since data points that remained were picked using the most objective standards, it can also be said that Vs variations in the Objective maps have a higher degree of confidence than the Subjective maps. This is indicated by RMS error maps showing that overall error values were reduced in the case of the Objective analysis. Therefore, both types of maps should be used during interpretation.

## CONCLUSIONS

By analyzing the fundamental-mode dispersion of Rayleigh waves, stiffness variations in soils were successfully mapped in both horizontal and vertical directions along the survey lines. A greater confidence is placed on the results from objective analyses in comparison to subjective analysis.

## REFERENCES CITED


Bullen, K.E., 1963, An introduction to the theory of seismology, 3rd ed.; Cambridge University Press, London, 381 pp.

Dobrin, M.B., and Savit, C.H., 1988, Introduction to geophysical prospecting, 4th ed.: McGraw-Hill, Inc., New York, 867 pp.

Lunne, T., 1997, Cone penetration testing in geotechnical practice; Blackie Academic & Professional, London, 312 pp.

Miller, R.D., Xia, J., Park, C.B., and Ivanov, J., 1999, "Multichannel analysis of surface waves to map bedrock," *The Leading Edge*, 18(12), 1392-1396.

Park, C.B., Miller, R.D., and Miura, H., 2002, Optimum field parameters of an MASW survey [Exp. Abs.]: SEG-J, Tokyo, May 22-23, 2002.

Park, C.B., Miller, R.D., and Xia, J., 2001, Offset and resolution of dispersion curve in multichannel analysis of surface waves (MSW): Proceedings of the SAGEEP 2001, Denver, Colorado, SSM-4.

Park, C.B., Miller, R.D., and Xia, J., 1999a, "Multi-channel analysis of surface waves," *Geophysics*, 64(3), 800-808.

Park, C.B., Miller, R.D., Xia, J., Hunter, J.A., and Harris, J.B., 1999b, Higher mode observation by the MASW method [Exp. Abs.]: Soc. Explor. Geophys., p. 524-527.

Park, C.B., Xia, J., and Miller, R.D., 1998, Imaging dispersion curves of surface waves on multi-channel record: 68th Ann. Internat. Mtg., Soc. Expl. Geophys., Expanded Abstracts, 1377-1380.

Richart, F.E., Hall, J.R., and Woods, R.D., 1970, Vibrations of soils and foundations: Prentice-Hall, Inc., 414 pp.

Sheriff, R.E., and Geldart, L.P., 1982, Exploration seismology, volume 1: Cambridge University Press, 253 pp.

Stokoe II, K. H., Wright, S.G., Bay, J.A., and Roesset, J.M., 1994, Characterization of geotechnical sites by SASW method, in Geophysical characterization of sites, ISSMFE Technical Committee #10, edited by R.D. Woods, Oxford Publishers, New Delhi.

*SurfSeis* v. 1.5, 2003, Users' Manual; Kansas Geological Survey, Lawrence, Kansas.

Telford, W.M., Geldart, L.P., Sheriff, R.E., and Keys, D.A., 1976, Applied Geophysics, Cambridge University Press, Cambridge, 860 pp.

Xia, J., Miller, R.D., and Park, C.B., 1999, "Estimation of near-surface shear-wave velocity by inversion of Rayleigh wave," *Geophysics*, 64(3), 691-700.

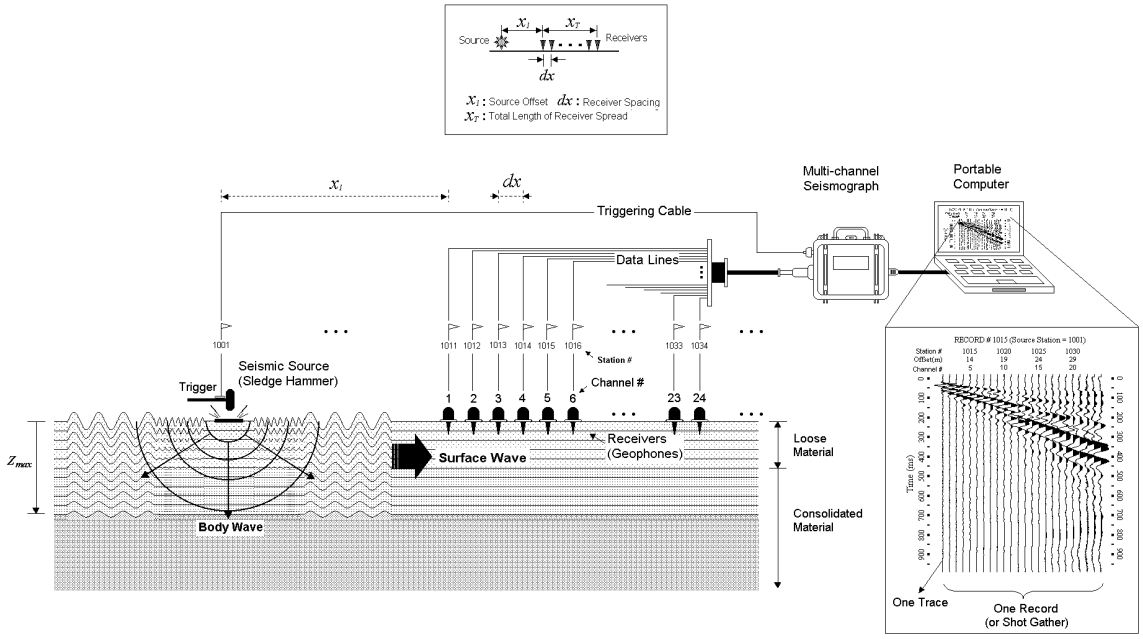


Figure 1. A schematic illustrating a typical field configuration with an MASW survey.

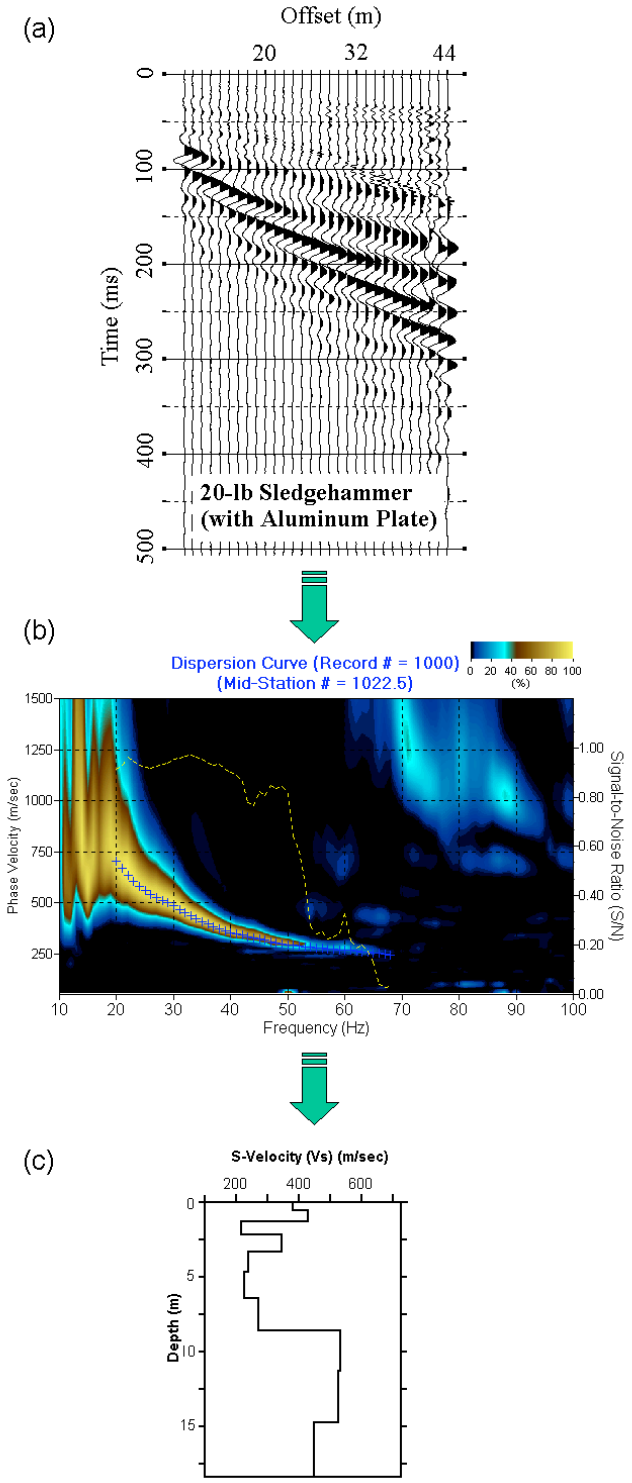


Figure 2. General procedure of MASW processing. A multichannel record (shot gather) in (a) is transformed into (b) an overtone image in which the fundamental-mode dispersion is identified and corresponding signal curve is extracted, and then (c) the curve is inverted into a 1-D Vs profile.

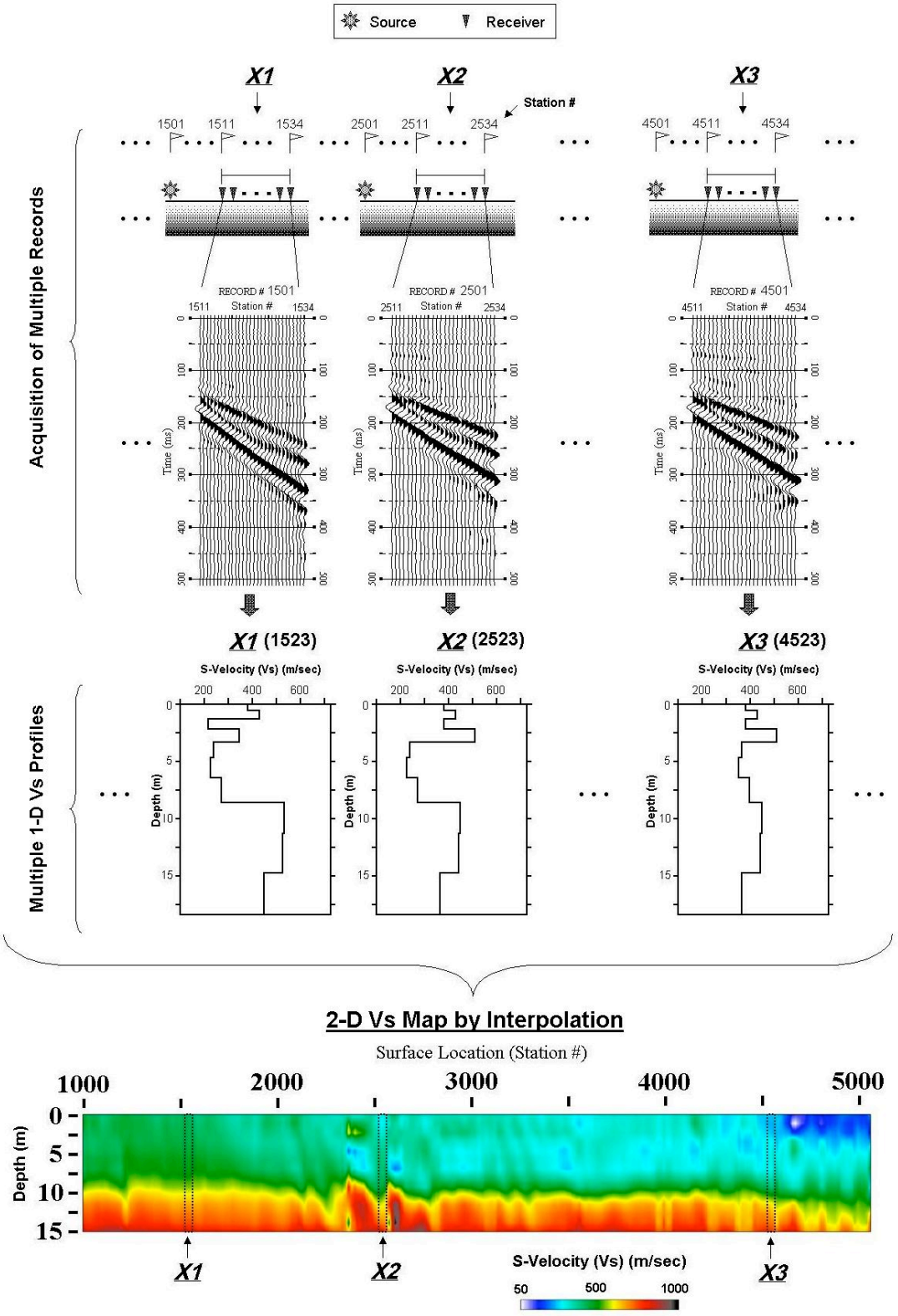


Figure 3. Illustration of the procedure to generate a 2-D Vs map from a roll-along mode MASW survey.

(a)

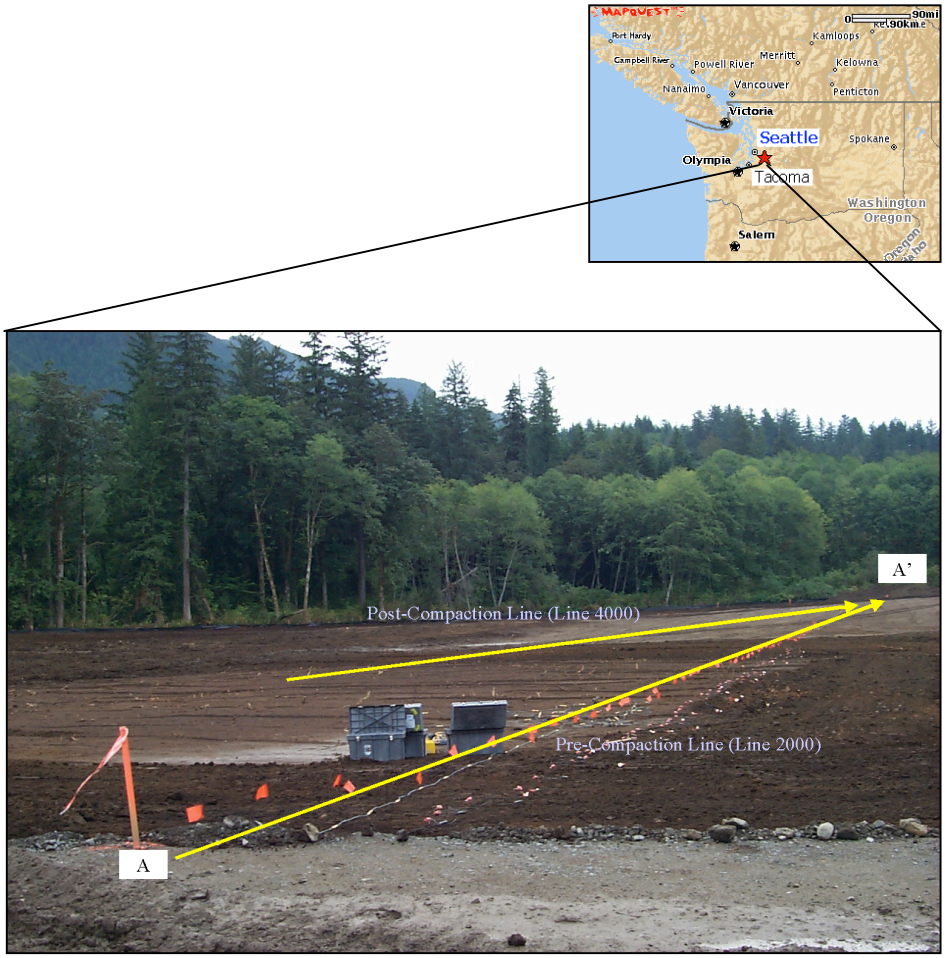


(b)

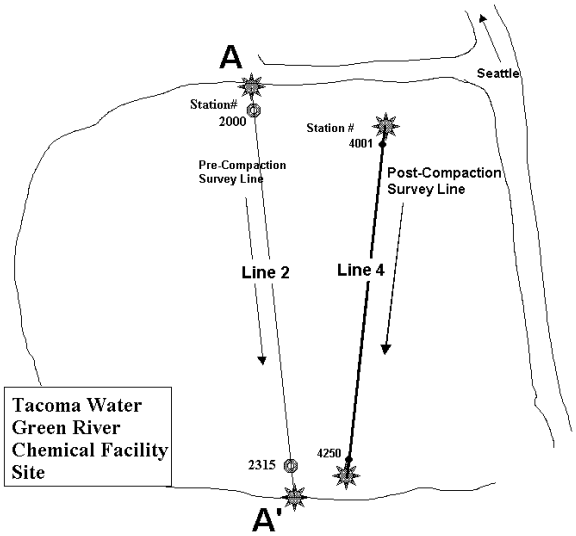


Figure 4. (a) General location of the site and (b) schematic of the two survey lines.

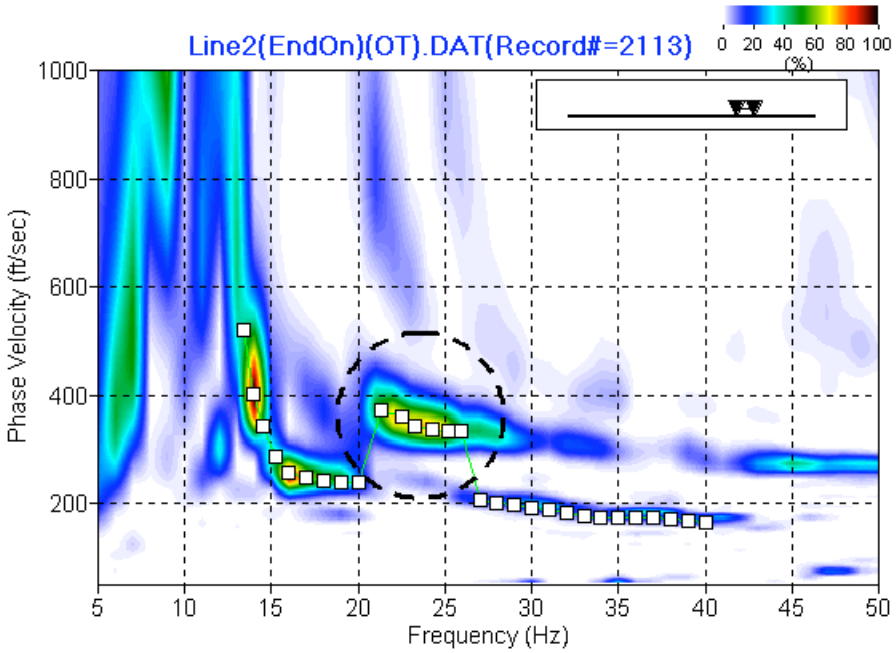


Figure 5. An example of dispersion curve extraction using *SurfSeis* that shows a higher mode adjacent to the fundamental mode causing some erroneous picking of phase velocities. In this instance the pickings would be manually edited.

(a)

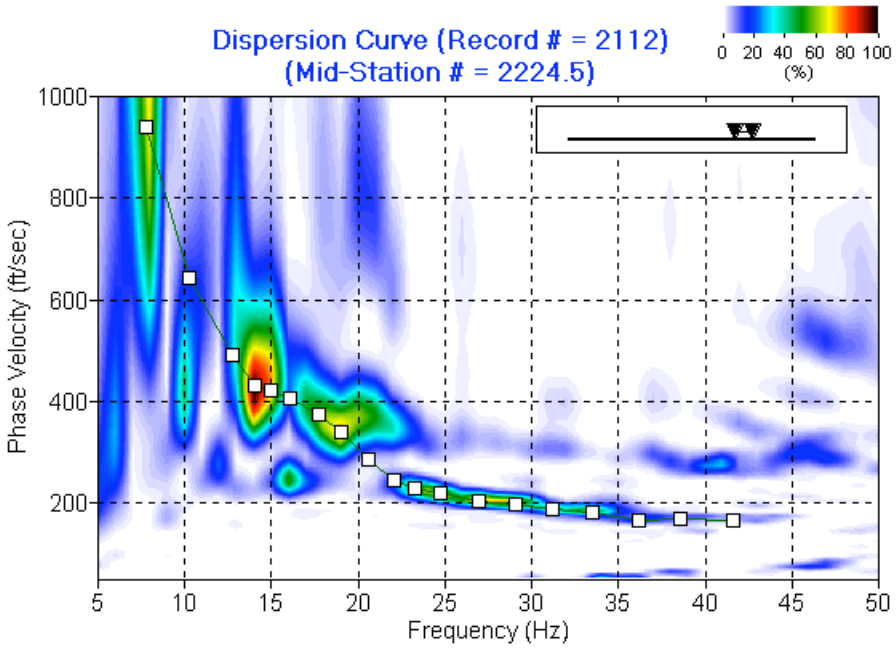


(b)

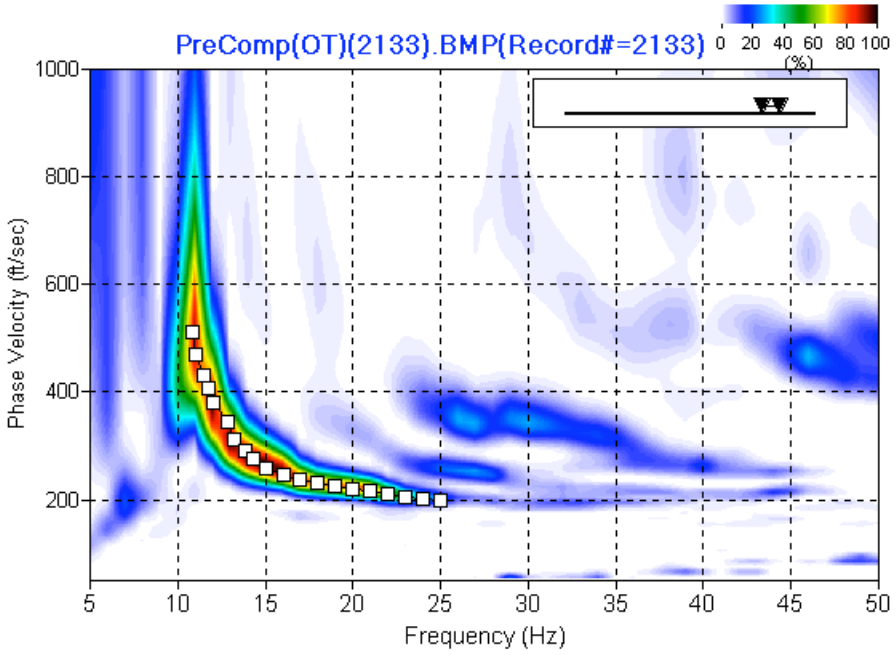


Figure 6. Examples of dispersion curve extraction based on the overtone image; (a) a curve is extracted with as much subjective judgment as possible (Subjective analysis) and (b) only by the objective trend of dispersion (Objective analysis).

(a)

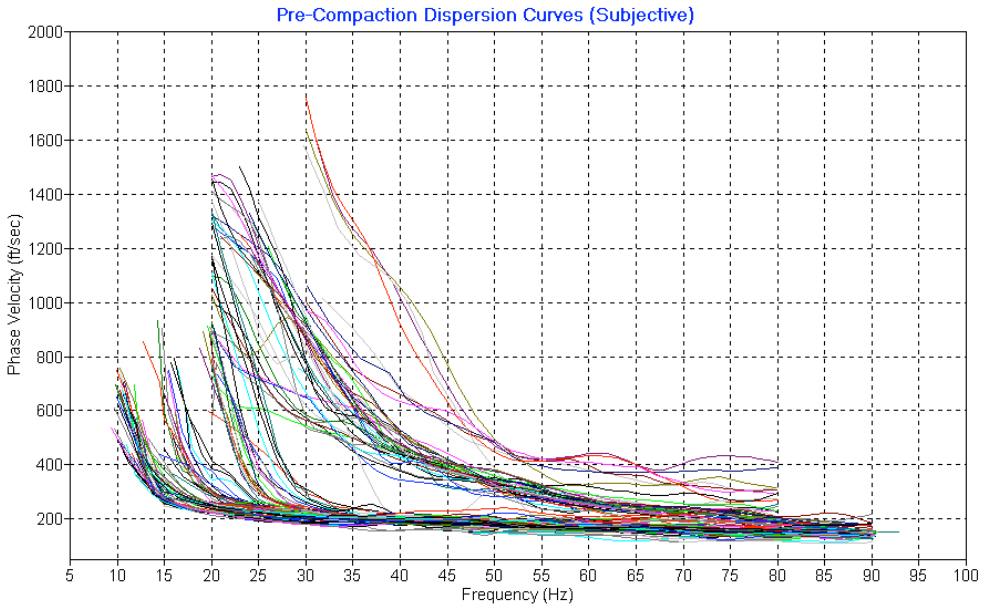


(b)

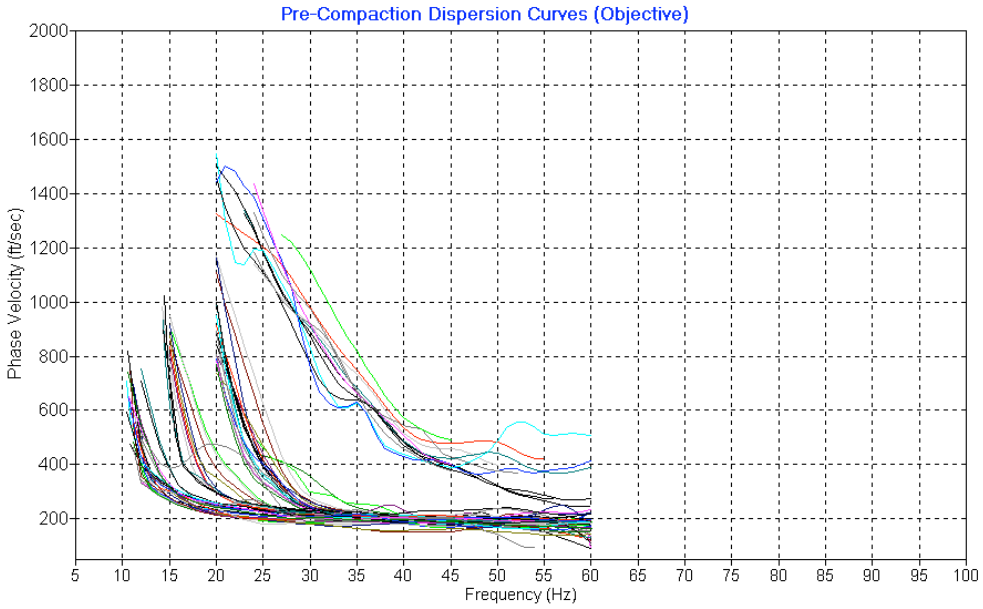


Figure 7. Display of dispersion curves extracted from (a) the Subjective and (b) the Objective analyses of the pre-compaction (line 2000) data.

(a)

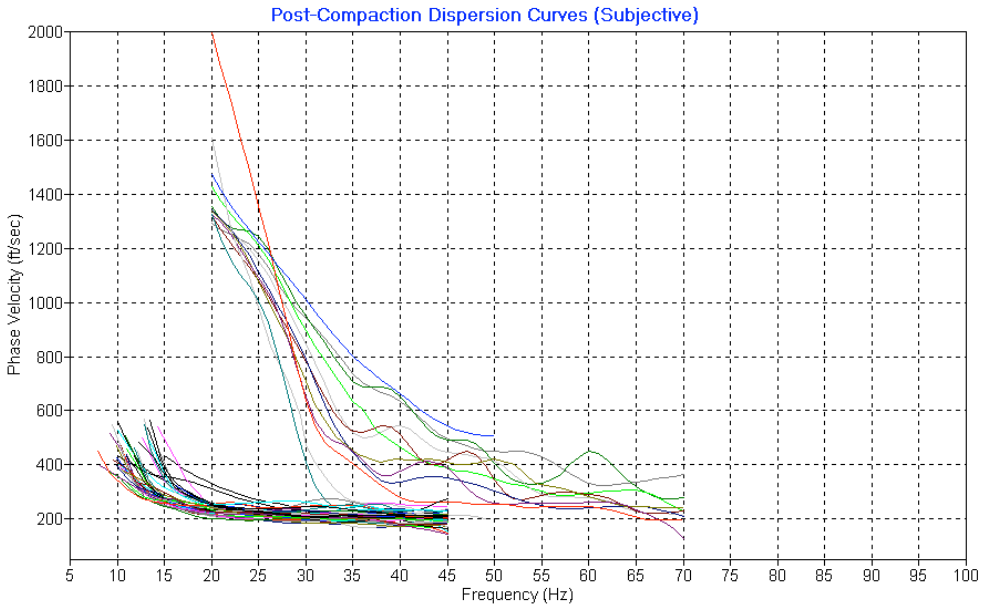


(b)

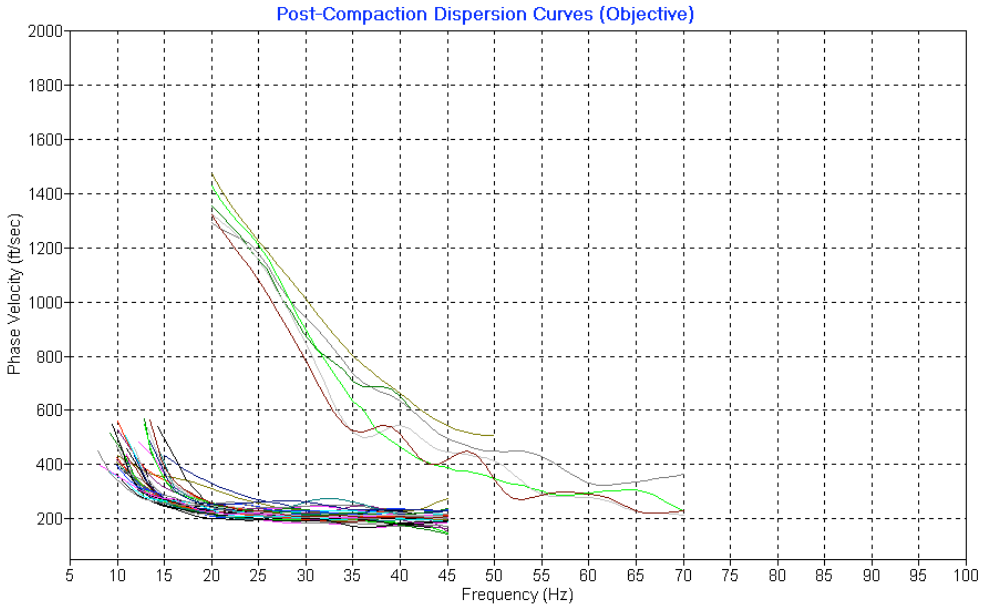


Figure 8. Display of dispersion curves extracted from (a) the Subjective and (b) the Objective analyses of the post-compaction (line 4000) data.

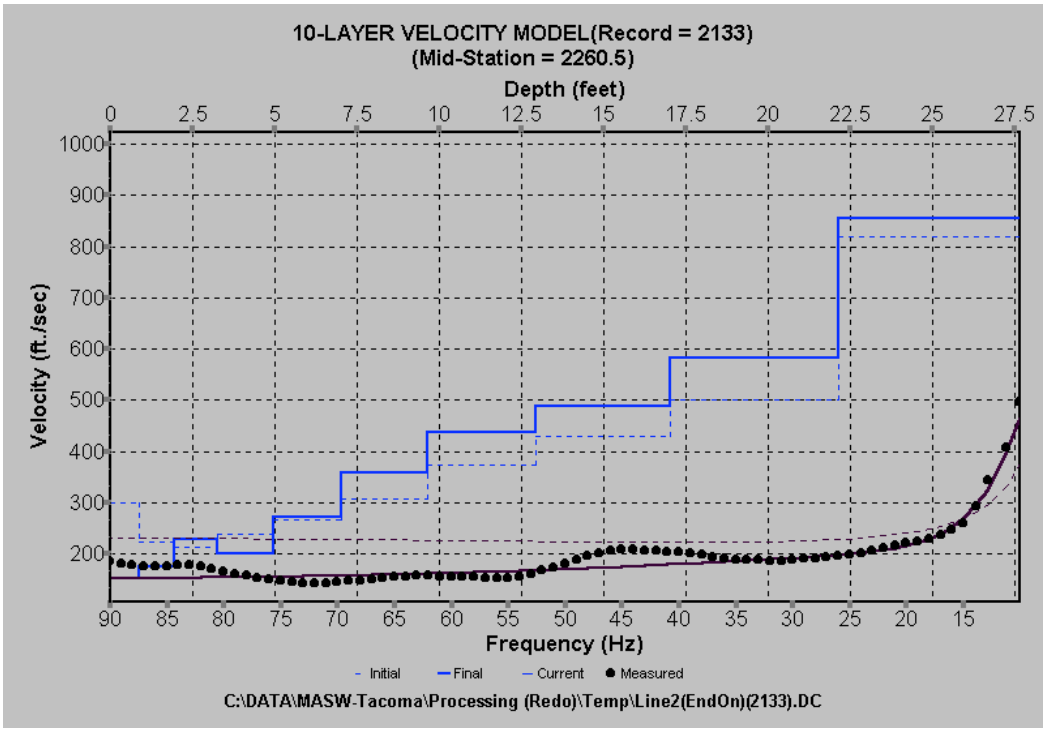


Figure 9. An example of inversion for a 1-D Vs profile in which a 10-layer depth model is created with varying thicknesses (increasing with depth) determined from the input dispersion curve (represented by dots).

(a)

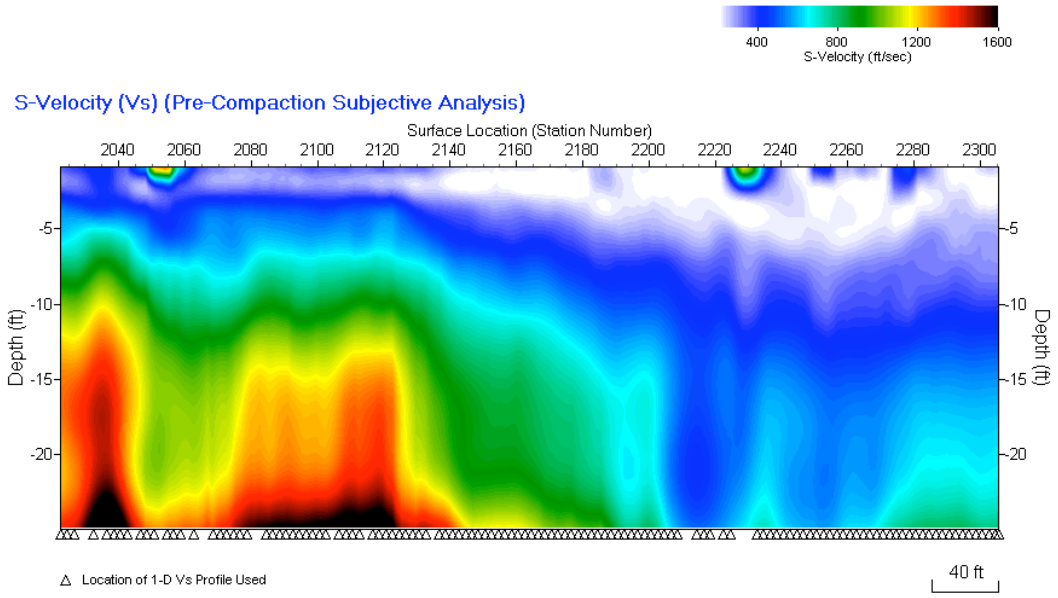


(b)

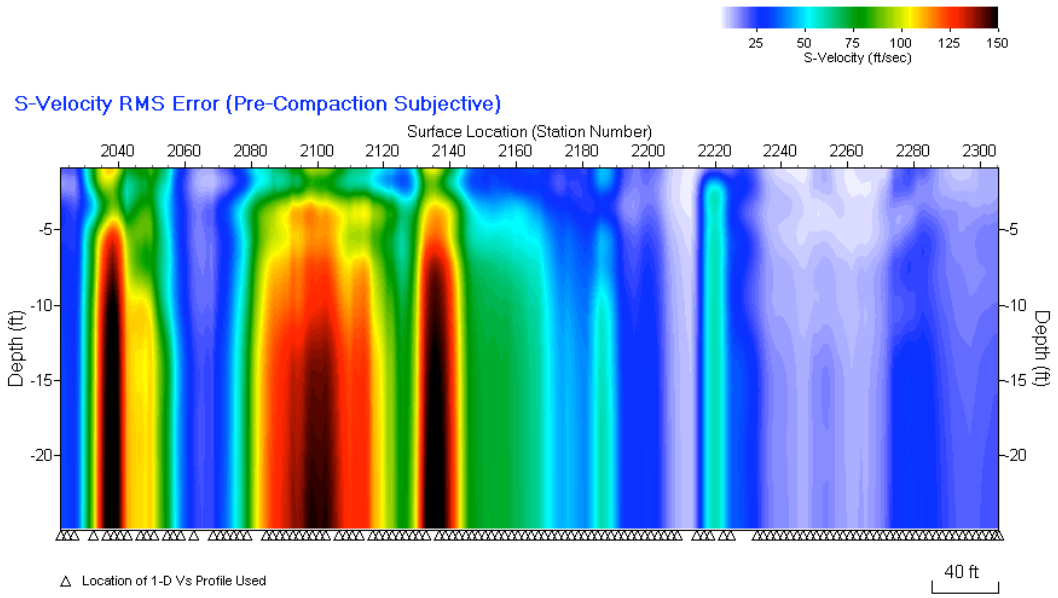


Figure 10. (a) Pre-compaction Vs map constructed from inversion of all Subjective dispersion curves and (b) the corresponding RMS-Error map.

(a)

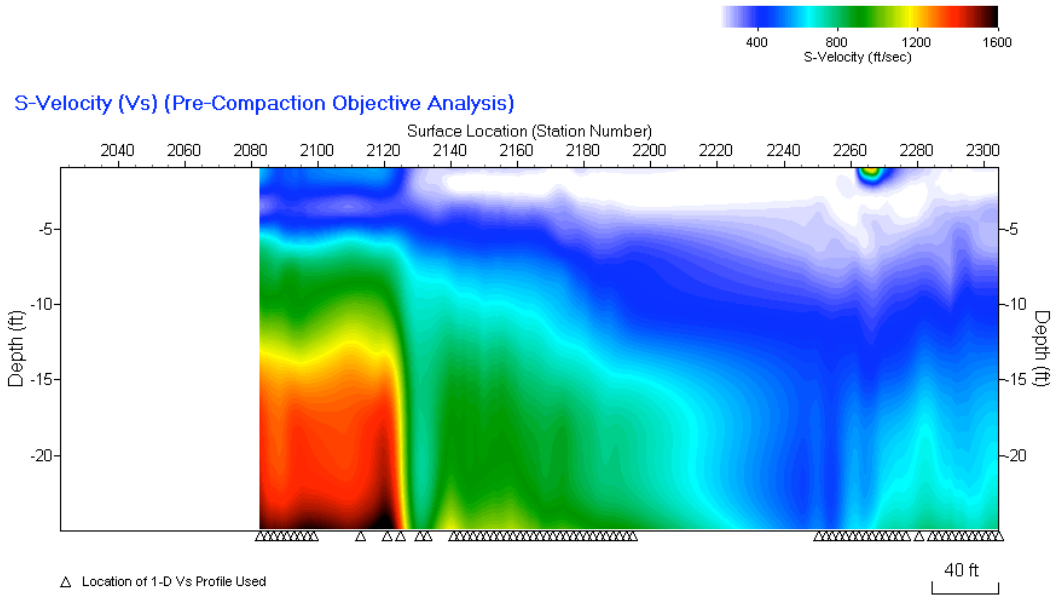


(b)

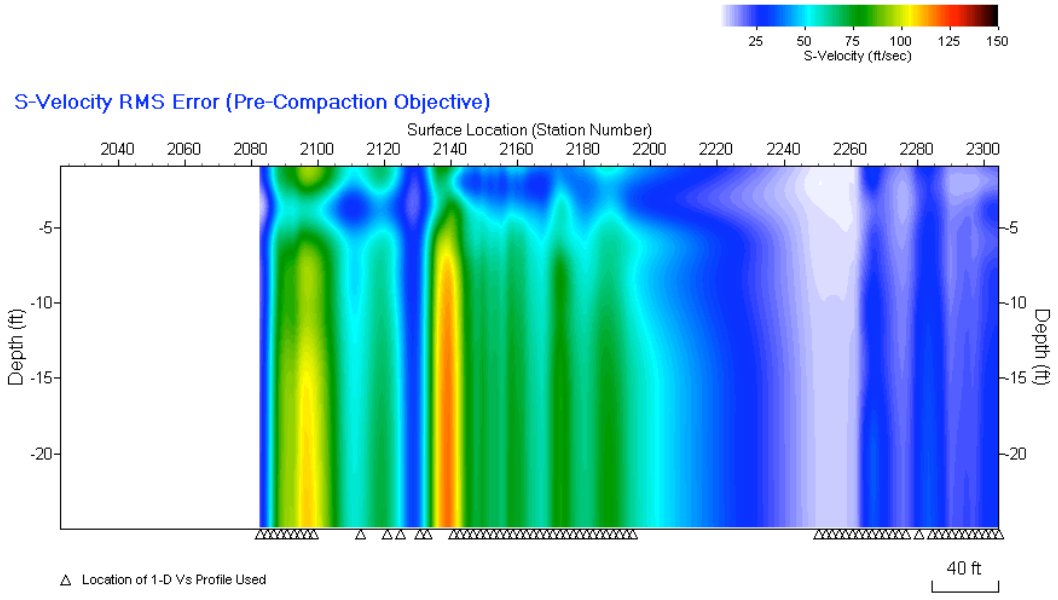


Figure 11. (a) Pre-compaction Vs map constructed from inversion of all Objective dispersion curves and (b) the corresponding RMS-Error map.

(a)

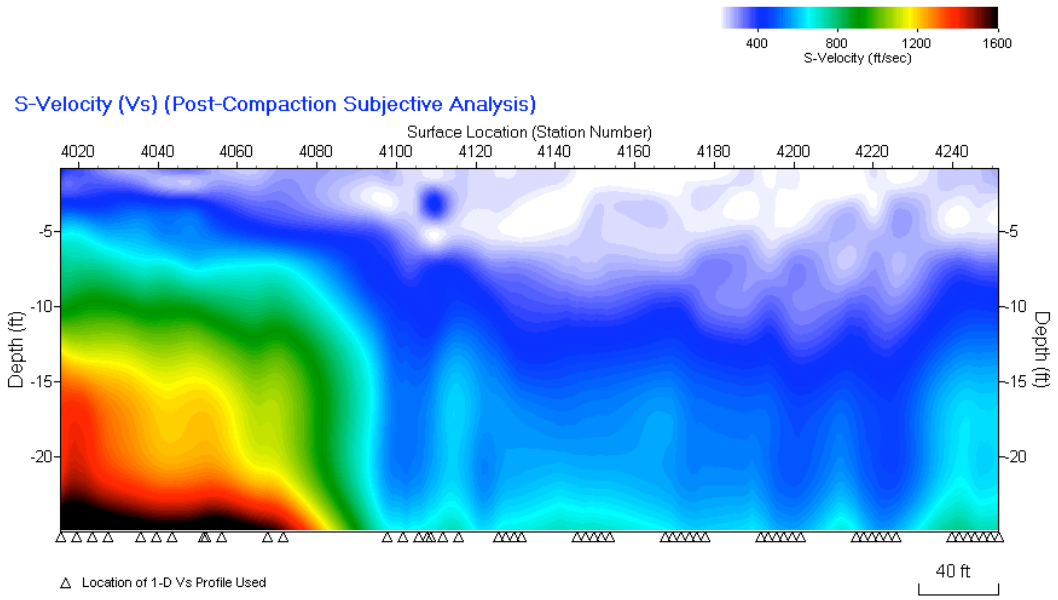


(b)

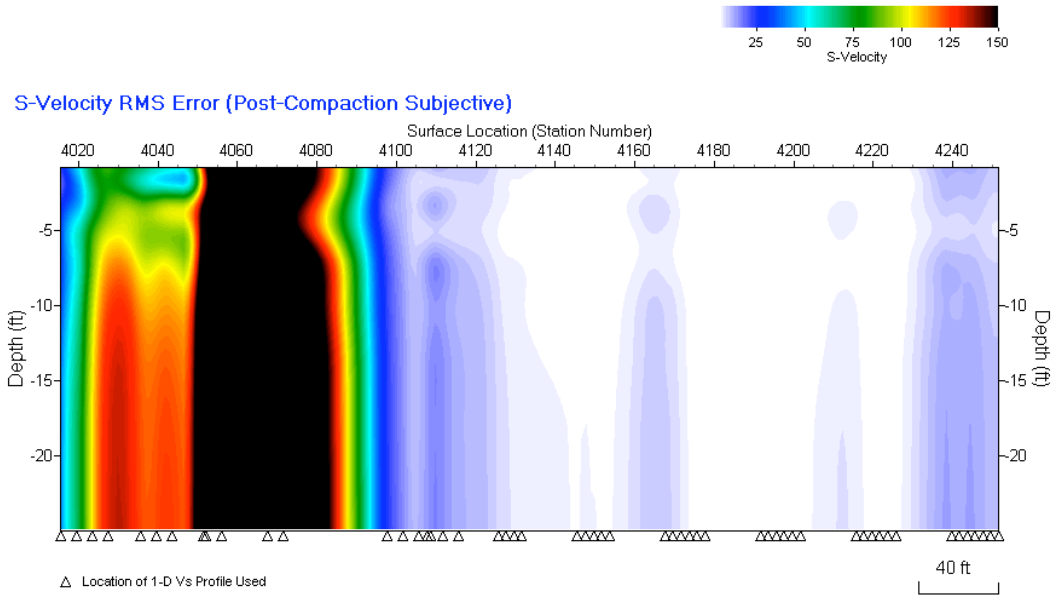


Figure 12. (a) Post-compaction Vs map constructed from inversion of all Subjective dispersion curves and (b) the corresponding RMS-Error map.

(a)

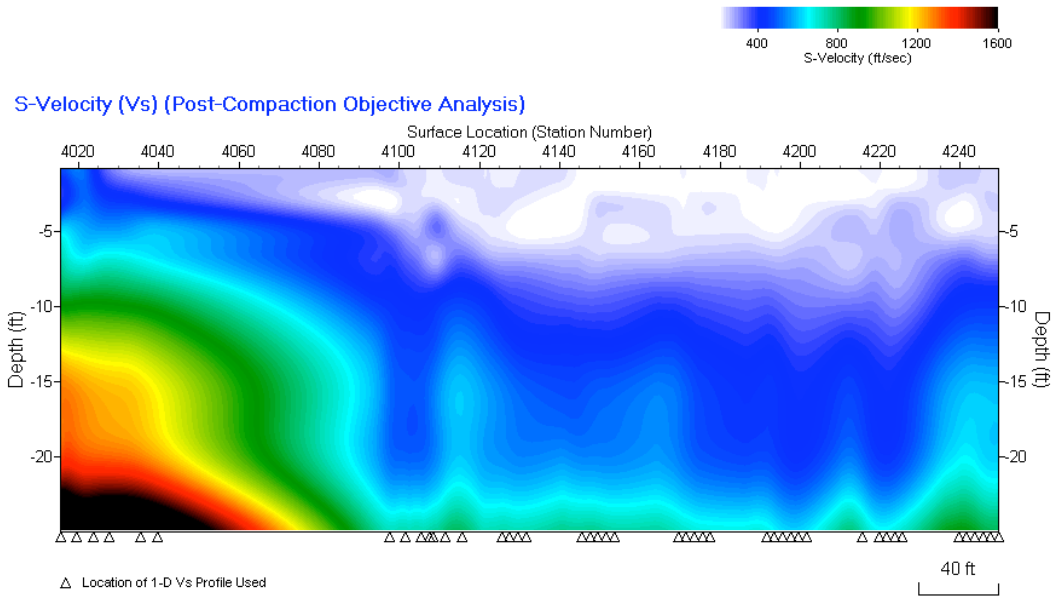


(b)

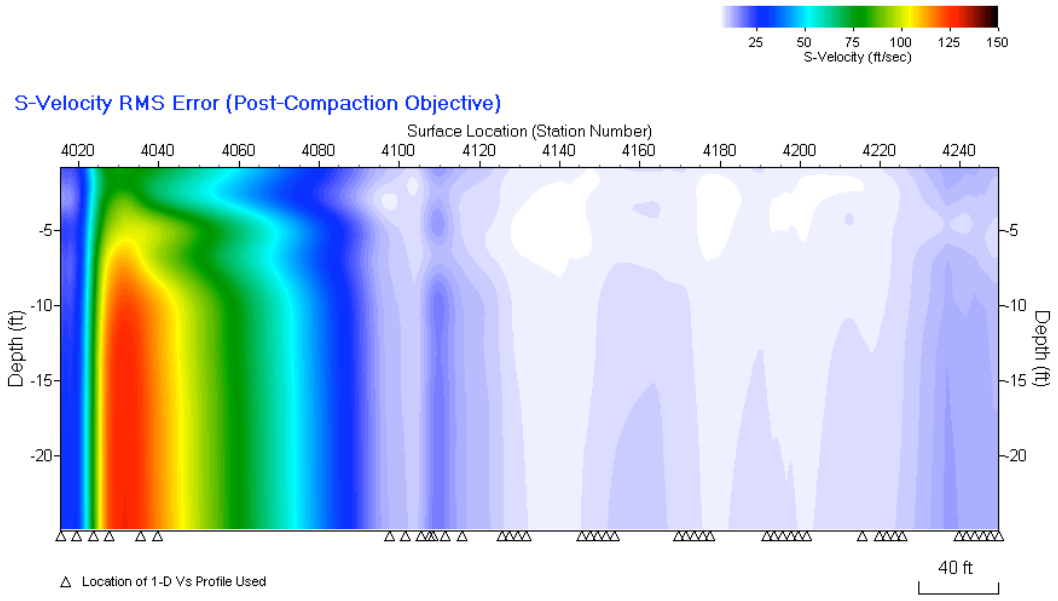


Figure 13. (a) Pre-compaction Vs map constructed from inversion of all Objective dispersion curves and (b) the corresponding RMS-Error map.